Discover 25+ Color Optimized Flow Cytometry Panels
- Human General Phenotyping Panel
- Human T Cell Differentiation and Exhaustion Panel
- Human T Cell Differentiation and CCRs Panel
Learn more
BioLegend®
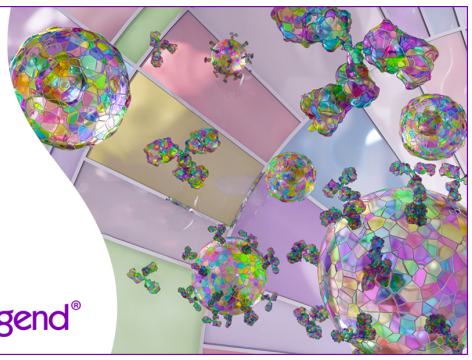

The Journal of Immunology
RESEARCH ARTICLE | AUGUST 01 2013

Regulation of Adaptive Immunity by the Fractalkine Receptor during Autoimmune Inflammation FREE

Jenny A. Garcia; ... et. al

J Immunol (2013) 191 (3): 1063–1072.
https://doi.org/10.4049/jimmunol.1300040

Related Content

The Fractalkine Receptor but Not CCR2 Is Present on Microglia from Embryonic Development throughout Adulthood
J Immunol (January,2012)

Fractalkine-Mediated Endothelial Cell Injury by NK Cells
J Immunol (April,2000)

Fractalkine Is an Epithelial and Endothelial Cell-Derived Chemoattractant for Intraepithelial Lymphocytes in the Small Intestinal Mucosa
J Immunol (March,2000)

Downloaded from http://www.jimmunol.org/jimmunol/article-pdf/191/3/1063/1379268/1300040.pdf by guest on 19 April 2024

Regulation of Adaptive Immunity by the Fractalkine Receptor during Autoimmune Inflammation

Jenny A. Garcia,* Paula A. Pino,* Makiko Mizutani,† Sandra M. Cardona,* Israel F. Charo,‡ Richard M. Ransohoff,† Thomas G. Forsthuber,*,§ and Astrid E. Cardona*,§

Fractalkine, a chemokine anchored to neurons or peripheral endothelial cells, serves as an adhesion molecule or as a soluble chemoattractant. Fractalkine binds CX3CR1 on microglia and circulating monocytes, dendritic cells, and NK cells. The aim of this study is to determine the role of CX3CR1 in the trafficking and function of myeloid cells to the CNS during experimental autoimmune encephalomyelitis (EAE). Our results show that, in models of active EAE, *Cx3cr1*$^{-/-}$ mice exhibited more severe neurologic deficiencies. Bone marrow chimeric mice confirmed that CX3CR1 deficiency in bone marrow enhanced EAE severity. Notably, CX3CR1 deficiency was associated with an increased accumulation of CD115^{+}Ly6C^{-}CD11c^{+} dendritic cells into EAE-affected brains that correlated with enhanced demyelination and neuronal damage. Furthermore, higher IFN-γ and IL-17 levels were detected in cerebellar and spinal cord tissues of CX3CR1-deficient mice. Analyses of peripheral responses during disease initiation revealed a higher frequency of IFN-γ– and IL-17–producing T cells in lymphoid tissues of CX3CR1-deficient as well as enhanced T cell proliferation induced by CX3CR1-deficient dendritic cells. In addition, adoptive transfer of myelin oligodendrocyte glycoprotein$_{35–55}$-reactive wild-type T cells induced substantially more severe EAE in CX3CR1-deficient recipients when compared with wild-type recipients. Collectively, the data demonstrate that besides its role in chemoattraction, CX3CR1 is a key regulator of myeloid cell activation contributing to the establishment of adaptive immune responses. ***The Journal of Immunology*****, 2013, 191: 1063–1072.**

Multiple sclerosis (MS) is a chronic, inflammatory demyelinating disease of the CNS causing significant neurologic disability in young adults. Supported by experimental evidence largely collected from its major model, experimental autoimmune encephalomyelitis (EAE), MS is considered for many in the field a predominantly T cell–mediated autoimmune disease. Although the exact cause of MS remains unsolved, CNS inflammation is a key component of the pathophysiology of MS. Whereas chemokines are known to promote tissue inflammation via recruitment of immune cells to these sites, recently it was shown that chemokine–chemokine receptors also participate in cellular activation and modulate effector functions of certain immune cell subsets (1, 2).

The discovery of the chemokine receptor CX3CR1 and its unique ligand fractalkine (CX3CL1) in the mid 1990s represented a major advancement in the understanding of myeloid cell function (3–5). Fractalkine is a distinct chemokine, expressed as a membrane-bound glycoprotein on neurons and peripheral endothelial cells (3, 6, 7). The fractalkine receptor (CX3CR1) is present on microglia and circulating monocytes, dendritic cells, and NK cells. Fractalkine, first known as neurotactin due to its abundant expression in the brain, plays different roles in different tissue compartments and disease states. We discovered that CX3CL1 signaling promotes microglial survival and controls microglial neurotoxicity through its unique receptor CX3CR1 under certain neurodegenerative and inflammatory conditions. Importantly, in humans, two single-nucleotide polymorphisms give rise to four allelic receptor variants. The most studied forms are CX3CR1$^{V249/T280}$ (also considered as the reference receptor) and the variant alleles CX3CR1$^{I249/T280}$ and CX3CR1$^{I249/M280}$ present in 20–30% of the population. These changes decrease fractalkine affinity and correlate with enhanced susceptibility to age-related macular degeneration (8, 9) and protection from atherosclerosis (10–12). Notably, a genetic study in a Serbian population (397 MS patients) found a significantly lower frequency of the CX3CR1$^{I249/T280}$ haplotype in secondary progressive compared with relapsing–remitting patients. Therefore, understanding the function of CX3CR1 during disease initiation will be valuable to understand the immune pathology of MS.

Monocytes and dendritic cells (13–15) are critical mediators of innate and adaptive immune responses. Notably, CX3CR1 distinguished a monocyte subset in peripheral blood so-called resident and phenotypically recognized as LFA-1^{+}/LSel^{-}/Ly6C^{-}/CCR2^{-}/CX3CR1^{high}, whereas the MCP-1 (or CCL2) receptor CCR2, marked inflammatory monocytes, distinguished as LFA-1^{-}/L-Sel^{+}/Ly6C^{+}/CCR2^{+}/CX3CR1^{low} (14, 16, 17). The recent characterization of red fluorescent protein (RFP)–CCR2 knock-in mice and the generation of mouse models carrying CX3CR1-GFP/

*Department of Biology, University of Texas at San Antonio, San Antonio, TX 78249; †Department of Neurosciences, Neuroinflammation Research Center, Lerner Research Institute, Cleveland Clinic, Cleveland, OH 44195; ‡Gladstone Institute of Cardiovascular Research, San Francisco, CA 94158; and §South Texas Center for Emerging Infectious Diseases, University of Texas at San Antonio, San Antonio, TX 78249

Received for publication January 7, 2013. Accepted for publication May 28, 2013.

This work was supported in part by National Multiple Sclerosis Society Grants RG3701 (to T.G.F.) and TA 3021 A1/T (to A.E.C.) and National Institutes of Health Grants NS-52177 (to T.G.F.) and SC1GM095426 (to A.E.C.).

Address correspondence and reprint requests to Dr. Astrid E. Cardona, One UTSA Circle, Margaret Batts Tobin Laboratory MBT 1.216, San Antonio, TX 78249. E-mail address: astrid.cardona@utsa.edu

The online version of this article contains supplemental material.

Abbreviations used in this article: CNTF, ciliary neurotrophic factor; EAE, experimental autoimmune encephalomyelitis; KO, knockout; MBP, myelin basic protein; MOG, myelin oligodendrocyte glycoprotein; MS, multiple sclerosis; PFA, paraformaldehyde; p.i., postimmunization; RFP, red fluorescent protein; WT, wild-type.

Copyright © 2013 by The American Association of Immunologists, Inc. 0022-1767/13/$16.00

Downloaded from http://www.jimmunol.org/jimmunol/article-pdf/191/3/1063/1379268/1300040.pdf by guest on 19 April 2024

CCR2-RFP reporter proteins provided additional support for a distinct molecular signature of CX3CR1 and CCR2 during embryonic development (18) and brain inflammation. CCR2 is critical for efficient accumulation of Ly6C^{high}/CCR2^{high} monocytes to the CNS. Furthermore, microglia in the adult naive and EAE-inflamed CNS were found CX3CR1^{high}/CCR2^{-} (19), and, similar to the populations described in peripheral blood, the EAE brain monocytes also appeared as CCR2^{high}CX3CR1^{low} or CCR2^{low} CX3CR1^{high} (19).

Due to the contrasting expression of CX3CR1 on the two major monocyte populations, we sought to investigate the role of CX3CR1 in accumulation of myeloid cells to the CNS during EAE and its effects on brain pathology. For this, we used *Cx3cr1*$^{GFP/GFP}$ (or *Cx3cr1*$^{-/-}$) mice and *Cx3cr1*$^{GFP/GFP}$*Ccr2*$^{+/RFP}$ and controls (*Cx3cr1*$^{+/+}$ and *Cx3cr1*$^{+/GFP}$*Ccr2*$^{+/RFP}$) to characterize myeloid cells in brain and lymphoid tissues at peak of EAE disease and investigate the role of these cells in promoting T cell activation and proliferation. Our results show that *Cx3cr1*$^{-/-}$ mice exhibited more severe neurologic signs. Radiation bone marrow chimeric mice confirmed that CX3CR1 deficiency in bone marrow enhanced EAE severity. Notably, CX3CR1 deficiency was associated with an increased accumulation of CD115^{+}/Ly6C^{-}/CCR2^{-} CD11c^{+} dendritic cells into EAE-affected brains that correlated with enhanced demyelination and neuronal damage. Wild-type (WT; *Cx3cr1*$^{+/+}$) infiltrating T cells showed an increased expression of IL-10 when compared with CX3CR1-deficient cells. Furthermore, higher IFN-γ and IL-17 levels were detected in cerebellar and spinal cord tissues of CX3CR1-deficient mice. Analyses of peripheral responses during disease initiation revealed a higher frequency of IFN-γ– and IL-17–producing T cells in lymphoid tissues of CX3R1-deficient as well as enhanced T cell proliferation induced by CX3CR1-deficient dendritic cells. Finally, adoptive transfer of myelin oligodendrocyte glycoprotein (MOG)$_{35–55}$-reactive WT T cells induced substantially more severe EAE in CX3CR1-deficient recipients when compared with WT recipients. Collectively, the data demonstrate that CX3CR1 is not only chemotactic, but a key regulator of myeloid cell activation contributing to the establishment of adaptive immune responses.

Materials and Methods

Mice

C57BL/6, *Cx3cr1*$^{GFP/GFP}$ (*Cx3cr1*$^{-/-}$), *Cx3cr1*$^{+/GFP}$*Ccr2*$^{+/RFP}$, and *Cx3cr1*$^{GFP/GFP}$*Ccr2*$^{+/RFP}$ mice were maintained at the Laboratory Animal Resources Unit at University of Texas at San Antonio. All experiments were performed in accordance with National Institutes of Health guidelines and approved by University of Texas at San Antonio Institutional Animal Care and Use Committee.

Mice were genotyped by PCR using DNA isolated from ear punch biopsies and chemokine receptor-specific primers, as previously described (1).

Active EAE induction

Active EAE was induced in mice 8–10 wk old by s.c. immunization with 100 μg MOG$_{35–55}$ peptide in CFA, as previously described (18). Mice were weighed and examined daily for EAE signs and scored as follows: 0, no signs of neurologic disease; 1, lack of tail tone; 2, abnormal gait, hind limb weakness; 2.5, partial hindlimb paralysis; 3, complete hindlimb paralysis; 3.5, ascending paralysis; 4, tetraplegia; and 5, death. Mice were sacrificed when they reached a score of 2.5–3.0 (1). Mice were sacrificed at disease initiation at 11 d postimmunization (p.i.), at peak of EAE disease (16–21 d p.i.), or 60 d p.i. (chronic phase).

Passive EAE induction

Mice were immunized with 300 μg MOG$_{35–55}$ peptide in CFA. Spleen and lymph nodes were harvested, and single mononuclear cell suspensions were prepared 10 d p.i. and cultured in the presence of 20 μg/ml MOG$_{35–55}$, 20 ng/ml murine rIL-23 (R&D Systems), and 10 μg/ml anti–IFN-γ (R4-6A2; BioXcell) in complete media (20–22). After 3-d incubation, cells were collected and washed in DMEM containing 50 μg/ml gentamicin, and 20–50 × 10^{6} cells were i.p. injected into WT or *Cx3cr1*$^{-/-}$ recipient mice. A separate aliquot of the isolated cells was subjected to IFN-γ and IL-17 cytokine ELISPOT assays. This was performed on primed T cell from WT and CX3CR1-knockout (KO) mice, to normalize the number of cells injected per recipient and compare similar number of effector cells per experiment. Prior to injection, recipients were injected with 200 ng pertussis toxin i.p. on the day of cell transfer and 48 h after transfer. Mice were weighed and EAE scored daily.

Generation of bone marrow chimeric mice

Recipient mice (5–6 wk old) were irradiated with a dose of 9 Gy and allowed to recover overnight before bone marrow reconstitution. Bone marrow cells were isolated from femur and tibia, as previously described (1). Briefly, mice were sacrificed by CO_2 asphyxiation, followed by cervical dislocation, and flushed bone marrow cells were resuspended in Iscove's media without FBS at 15 × 10^{7} cells/ml. Recipient mice were anesthetized 1–2 min (or until animals' loss of righting reflexes) in an induction chamber with oxygen flow rate of 1 L/min and isofluorane delivery to 3–4%, and 15–20 × 10^{6} cells were injected via the retro-orbital sinus in a volume of 100–150 μl. Mice were placed in a clean cage and monitored until righting reflex was gained. Six weeks after reconstitution, EAE was induced. Efficiency of engraftment was confirmed by flow cytometry 4 wk after bone marrow reconstitution by virtue of CD45.1 and CD45.2 congenic markers in donor and recipients, respectively.

Isolation of mononuclear cells and flow cytometry

Perfused brains and spinal cord tissues were dissected from mice at peak of EAE disease; mononuclear cells were separated over discontinuous 70/30% Percoll gradients, as previously described (23); and cellular pellets were resuspended in cell-staining buffer (BioLegend, San Diego, CA). Blood for single-stained controls was collected from the submandibular vein, and RBCs were depleted by hypotonic lysis and washed in staining buffer. Isolated cells were incubated on ice for 5 min with anti-mouse CD16/CD32 (clone 2.4G2; BD Pharmingen) to block FcRs and then incubated on ice for 30 min with a mix of fluorochrome-conjugated anti-mouse Abs, as follows: CD45-PerCP, allophycocyanin-Cy7, or allophycocyanin (clone 30-F11; BD Pharmingen); CD115-PE (clone AFS98; eBioscience); CD11b-PE (clone M1/70); CD11c-PeCy7 (clone N418; eBioscience); Ly6C-Alexa 647 (clone ER-MP20; AbD Serotec); CD80-allophycocyanin (clone 16-10A1); CD86-PerCP (clone GL-1); and I-A/I-E–Pacific Blue (mouse MHC-II clone M5/114.15.2). After washes, cells were resuspended in 2% paraformaldehyde and analyzed in a LSR-II (BD Biosciences, Franklin Lakes, NJ). Similar analyses were carried out in cell suspensions from lymph node and spleens at 11 d p.i. Lymphoid tissues were passed through a 70-μm nylon mesh, and spleen RBCs were depleted by hypotonic lysis prior to flow cytometry.

To quantify the proportion of resident and infiltrating myeloid cells undergoing cell proliferation, CNS mononuclear cells were stained with a mix of CD45-allophycocyanin (clone 30-F11) and CD11b-PerCP (clone M1/70) Abs for 30 min on ice, fixed with 4% paraformaldehyde (PFA) for 30 min, and then incubated at room temperature for 10 min in permeabilization buffer (eBioscience). Cells were then stained with Ki67-V450 (clone B56) in permeabilization buffer for 20 min, washed, resuspended in 2% PFA, and acquired on an LSRII. Flow cytometry data are presented as number or percentage of cells, or as mean fluorescence intensity for MHC-II, CD80, and CD86 markers.

Immunohistochemistry staining of brain sections

Following buffer perfusion, mice were perfused with 4% PFA. Dissected tissues were postfixed 24–36 h in 4% PFA and cryoprotected in 20% glycerol in 80 mM phosphate buffer (pH 7.6) for 48 h at 4°C. Free-floating 30-μm sections were prepared using a freezing microtome and stored at −20°C until use (2). After blocking, tissues were stained overnight at 4°C with anti-mouse CD45 Abs (clone IBL-3/16; AbD Serotec, Raleigh, NC), anti-mouse NeuN (clone A60; Millipore, Billerica, MA), anti-calbindin mAb (clone C26D12; Millipore), or anti–myelin basic protein (MBP) Ab (Invitrogen). Tissues were then incubated with biotin-labeled secondary Ab, and developed with avidin-biotin peroxidase system (Vector Laboratories, Burlingame, CA) with diaminobenzidine as a substrate (Invitrogen, Carlsbad, CA). Tissues were then mounted onto superfrost plus slides, allowed to air dry, and baked at 50°C for 20 min. Slides were then cleared in xylene and mounted using Permount reagent. After tissues were mounted onto slides, sections were stained with anti-CD45 Abs and subjected to Nissl staining. For this, sections were hydrated on graded

Downloaded from http://www.jimmunol.org/jimmunol/article-pdf/191/3/1063/1379268/1300040.pdf by guest on 19 April 2024

ethanol solutions (100, 95, and 70%) and stained for 3 min in 0.5% solution of cresyl violet, followed by dehydration (70, 95, and 100% ethanol). To assess differences, myelin content, three tissue sections per mouse ($n = 4$ per group), was imaged, and the area of myelin immunoreactivity in eight random images per section was obtained using Image-Pro Plus 6.2.1 (Media Cybernetics) in a blinded manner. Similarly, calbindin-positive cells were counted in 10 randomly acquired images per section in 3 different tissues per mouse. Individual cells were counted using the count analysis tool in Adobe Photoshop extended CS4 v11 (Adobe).

T cell proliferation assay

Mice immunized with 300 μg $MOG_{35–55}$ in CFA were sacrificed 11 d p.i. T cells were enriched from spleens by magnetic negative selection (Stemcell Technologies). For dendritic cell isolation, spleens were extracted and dissociated in spleen dissociation media (Stemcell Technologies) and enriched for $CD11c^+$ cells (Stemcell Technologies). T cells were labeled with the proliferation dye CFSE (eBioscience) and plated in complete media with 20 μg $MOG_{35–55}$ at 1×10^6 cells/well in a 96-well plate. Either CX3CR1 WT or KO $CD11c^+$ cells were added to the T cells at an equal ratio, and then the cells were incubated at 37°C for 3 d. Cells were labeled with viability dye eFluor780 (eBioscience), and then blocked with CD16/CD32 (BD Pharmingen) and labeled with a mixture of Abs for flow cytometrical analysis using LSR II.

Cytokine ELISPOT assay

Mice were immunized with 100 μg $MOG_{35–55}$ and sacrificed 11 d p.i. Spleen and lymph nodes were harvested and cells were plated at 1×10^6 per well with 10 μg/ml $MOG_{35–55}$ in complete HL-1 serum-free media in a 96-well filter plate that was previously sensitized with purified capture anti–IL-17 (clone 17CK15A5; eBioscience) or anti–IFN-γ (clone AN-18; eBioscience) and blocked with 1× PBS/1% BSA. After 24 h of incubation at 37°C/5% CO_2, the cells were washed with 0.5% Tween 20 in PBS, then labeled with biotin anti–IL-17 detection Ab (clone eBio17B7) or biotin anti–IFN-γ detection Ab (clone R4-6A2), and incubated at 4°C overnight. The cells were then incubated for 2 h at room temperature with streptavidin alkaline phosphatase (Invitrogen) diluted in PBS containing 1% BSA/0.5% Tween 20 and developed with 5-bromo-4-chloro-3-indolyl phosphate/NBT phosphatase substrate (KPL). Plates were read, and spots were counted using ImmunoSPOT software. Similarly, IFN-γ– and IL-17–producing cells were assayed in total brain leukocyte populations (isolated via Percoll gradients, as described above) from WT and CX3CR1-KO mice at peak of EAE disease. Number of spots in nonstimulated control wells was subtracted from the stimulated well, and data are presented as spot-forming cells per total million of cells added in the assay.

Quantitative RT-PCR

Tissues were dissected from perfused mice at the peak of EAE disease. Cerebellum was carefully detached using a scalpel and stored separately from forebrain and spinal cord tissues. Total RNA was isolated using TRIzol reagent, according to the manufacturer's instructions. Quantity was assessed with a Nanodrop 1000, and RNA quality was confirmed over 1% agarose gels. RNA was transcribed using TaqMan reverse-transcription reagents. Quantitative real-time PCR was performed with TaqMan Master mix and gene expression assay. Samples were analyzed on an Applied Biosystems 7900HT thermal cycler. All TaqMan reagents were from Applied Biosystems. Reactions were run in triplicates, and expression levels were normalized to β-actin.

Statistical analysis

Data are presented as mean ± SEM. Transcript data for IL-17 were analyzed using ANOVA. For all other experiments, differences between groups were analyzed using an unpaired t test with GraphPad Prism software (San Diego, CA). The p values are shown in the data, as follows: $^*p < 0.05$, $^*p > 0.01$, $^{**}p < 0.01$.

Results

Peripheral CX3CR1 deficiency confers more severe EAE

Two mouse models of CX3CR1 deficiency were reported in the earlier 2000s (24, 25). In mixed 50:50 hybrids of the C57BL/6 and 129/Sv strains, $Cx3cr1^{-/-}$ mice upon active immunization with $MOG_{35–55}$ peptides revealed a slightly earlier disease onset (24, 26, 27). A different study using mutant mice engineered by disrupting the CX3CR1 locus by insertion of the GFP reporter protein showed that CX3CR1-deficient mice on the $CD1d^{+/+}$ and $CD1d^{-/-}$ background developed EAE disease with earlier onset and correlated with a selective deficiency of NK cells in the CNS (28). Due to the expression of CX3CR1 by distinct monocyte/macrophage populations (18, 19), we sought to extend these studies and characterize the myeloid compartment in the CNS during EAE in the absence of CX3CR1 signaling. To begin to address this issue, active EAE was induced in $Cx3cr1^{GFP/GFP}$ ($Cx3cr1^{-/-}$, KO) mice backcrossed to the C57BL/6J background for >14 generations and WT littermates via s.c. injection of 100 μg $MOG_{35–55}$ peptide, and the mice were observed for EAE disease. All mice developed signs of EAE (Fig. 1A). However, CX3CR1-deficient mice showed EAE signs at an earlier time point (Fig. 1B). The peak of disease was also manifested earlier in $Cx3cr1^{-/-}$ mice (Fig. 1B), and the EAE signs were significantly more severe in the absence of CX3CR1, as shown by the comparison of maximum EAE scores between the groups (Fig. 1A, 1C). To delineate the contribution of peripheral versus CNS-resident cells to disease progression, we generated radiation bone marrow chimeric mice and active EAE was induced and monitored, as described earlier. Reconstitution of WT or $Cx3cr1^{-/-}$ recipient mice with $Cx3cr1^{-/-}$ bone marrow (KO→WT and KO→KO) showed a severe and nonremitting form of EAE, with a high proportion of mice exhibiting ascending paralysis that was sustained up to 45–50 d p.i. (Fig. 1D, 1E). Peak EAE was comparable in WT→KO and KO→WT chimeric mice (Fig. 1D); however, recipients of KO bone marrow failed to recover from EAE, whereas recipients of WT bone marrow (WT→KO) exhibited a progressive recovery, and motor function was regained in both hind limbs. Control bone marrow chimeric mice (WT→WT and KO→KO; Fig. 1E) showed a similar EAE phenotype in which the genotype of the circulating bone marrow–derived cells correlates with neurologic disease, as observed in the mixed chimeric mice (Fig. 1D). Overall, the results show that EAE severity observed in CX3CR1-deficient mice was due to absence of fractalkine signaling on peripheral bone marrow–derived cells.

Increased severity of CNS pathology in CX3CR1-deficient mice correlates with the increased accumulation of dendritic cells in the CNS

To investigate the mechanism underlying the increased severity of EAE in the absence of CX3CR1 signaling, we examined CNS inflammation at the time of peak disease in CX3CR1-KO mice also carrying the CCR2-RFP reporter protein. Heterozygous mice with normal receptor function ($Cx3cr1^{+/GFP}Ccr2^{+/RFP}$) and CX3CR1-deficient mice carrying the CCR2-RFP reporter ($Cx3cr1^{GFP/GFP}$ $CCR2^{+/RFP}$) were investigated for the accumulation of monocyte subsets upon active EAE induction (Fig. 2A, 2B). Myeloid subsets in the CNS were distinguished by flow cytometry using Abs against CD45 to distinguish $CD45^{high}$ infiltrating leukocytes from $CD45^{low}$ microglial cells. $CD45^{high}$ cells were further analyzed for the monocyte marker CD115 expression and $CD115^+$ cells for Ly6C and CD11c expression. The results show that, in heterozygous mice, >85% of $CD115^+$ monocyte-lineage cells were $Ly6C^{high}$ (also $CCR2^{high}$ by virtue of RFP expression), indicating a predominant infiltration of this population to the CNS during EAE, demonstrating the importance of CCR2 for recruitment of this subset into the CNS. In contrast, accumulation of the $Ly6C^{low}$ population was dramatically increased in the absence of CX3CR1 (Fig. 2B), and 60% of these cells also expressed the CD11c marker characteristic of dendritic cells. The population of $Ly6C^-$ $CD11c^+$ cells expressed CX3CR1 as revealed by comparison of CX3CR1-GFP and CCR2-RFP fluorescence intensities in the various myeloid populations. $Ly6C^{low}$ cells expressed higher

Downloaded from http://www.jimmunol.org/jimmunol/article-pdf/191/3/1063/1379268/1300040.pdf by guest on 19 April 2024

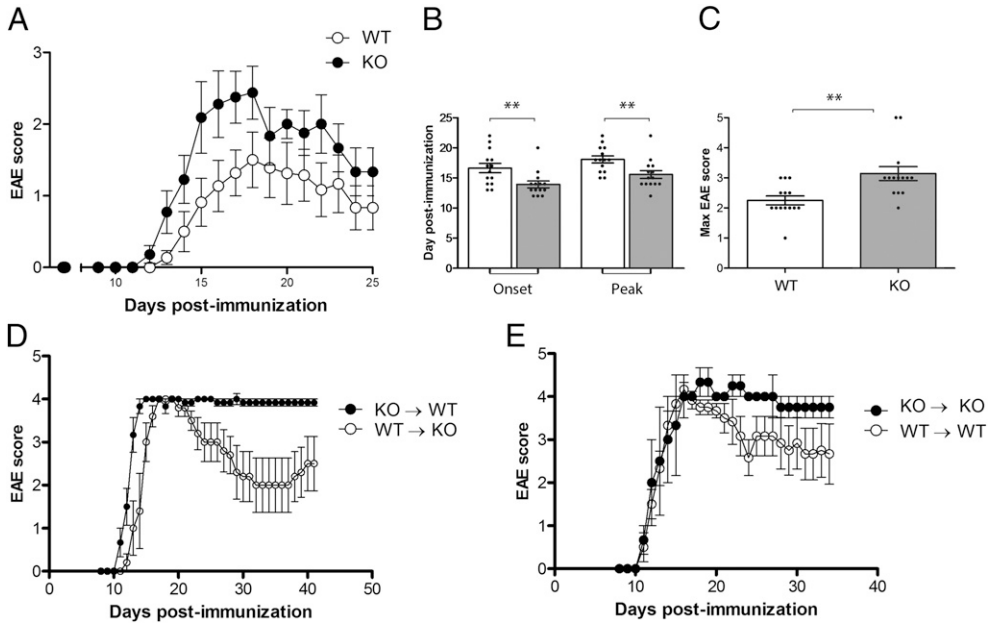

FIGURE 1. CX3CR1-deficient mice exhibit earlier disease onset and worse EAE disease. (**A**) *Cx3cr1*$^{-/-}$ (gray bars) and *Cx3cr1*$^{+/+}$ mice (open bars) were immunized with $MOG_{35–55}$ peptide and scored daily for neurologic signs. (**B**) Days of EAE onset and peak disease. (**C**) Maximum EAE score, $n = 14$ (*Cx3cr1*$^{+/+}$ mice) and $n = 15$ (*Cx3cr1*$^{-/-}$ mice). (**D**) Radiation bone marrow chimeras WT→KO ($n = 8$) and KO→WT ($n = 10$) and respective controls (**E**) WT→WT ($n = 7$) and KO→KO ($n = 7$) were immunized with $MOG_{35–55}$ peptide and scored daily. $^{**}p < 0.01$.

levels of CX3CR1 than Ly6C^{high} cells (Fig. 2C, $p = 0.008$ for comparison of CX3CR1-GFP expression between Ly6C^{+}CD11c^{+} and Ly6C^{-}CD11c^{+} cells; $p = 0.016$ for comparison of CCR2-RFP between Ly6C^{+}CD11c^{+} and Ly6C^{-}CD11c^{+} groups; $p = 0.046$ for comparison of CX3CR1-GFP and CCR2-RFP expression within Ly6C^{+}CD11c^{+} population; and $p = 0.008$ for comparison of CX3CR1-GFP and CCR2-RFP expression within Ly6C^{-}CD11c^{+} population). These results suggest that Ly6C^{high}/CCR2^{+} and Ly6C^{low}/CX3CR1^{+} subsets represent distinct populations with specialized functions within the CNS.

To establish a relationship between the infiltration of myeloid cells and CNS pathology, brains were sectioned and analyzed at the peak of EAE by immunohistochemistry. Tissues were stained with Abs against CD45, as a generalized marker of inflammation (Fig. 2D–F), MBP to assess demyelination (Fig. 2G–I), and calbindin as a marker for Purkinje cells in cerebellar regions (Fig. 2J–L). When compared with naive CX3CR1-KO tissues (Fig. 2D), infiltration of peripheral cells was evident in diseased WT mice (Fig. 1E) and CX3CR1-KO tissues. However, CD45 immunoreactivity was found most dramatic in forebrain and cerebellar white matter of CX3CR1-KO mice (Fig. 2F, Supplemental Figs. 1, 2). Myelin staining revealed a defined pattern in naive (Fig. 2G) and diseased WT mice (Fig. 2H), with myelin fibers darkly stained and axons easily visualized. In WT tissues affected by EAE, strong myelin immunoreactivity is observed in areas close to inflammatory cuffs (Fig. 2H). In contrast, CX3CR1-KO tissues revealed a decreased intensity in the myelin staining; axons appeared thinner and shorter, and less defined axons were visualized in the cerebellar region (Fig. 2I). Purkinje cells were detected along the granular cell layer of naive mice (Fig. 2J) and diseased WT mice (Fig. 2K). In contrast, in CX3CR1-KO mice, calbindin-positive neurons appeared with an altered morphology. Deteriorated/degenerating cells were evident by the presence of a disrupted lining of the granular cell layer, and ovoids at the ends of the axons were clearly visualized (Fig. 2L, Supplemental Fig. 1). Quantification of myelin immunoreactive area shows that naive CX3CR1-KO mice do not differ from naive WT mice (Fig. 2M). Similar results were found when assessing the number of calbindin-positive neurons (Fig. 2N). However, upon EAE induction, a reduction in both myelin (Fig. 2M, $^{*}p = 0.03$ between WT naive and WT-EAE groups, $p = 0.0002$ between KO naive and KO-EAE groups, and $^{**}p < 0.0001$ between WT-EAE and KO-EAE groups) and neuronal counts was detected with CX3CR1-KO mice revealing a more dramatic reduction when compared with diseased WT mice (Fig. 2N, $^{*}p = 0.04$ between WT-EAE and KO-EAE, and $p = 0.021$ between KO naive and KO-EAE groups). Therefore, the results indicate that an increased inflammatory reaction, dominated by a myeloid subset with a CD115^{+}Ly6C^{low} CD11c^{+} phenotype, correlated with enhanced demyelination and neuronal damage in CX3CR1-KO mice.

Differential cytokine expression in CX3CR1-KO mice is indicative of an increased proinflammatory environment in the CNS

To further examine mechanisms by which this myeloid subset conferred CNS pathology, we sought to investigate the frequency of IFN-γ and IL-17 $MOG_{35–55}$-specific producing T cells in the periphery. For this, we used lymph nodes and spleen tissues from actively immunized WT and CX3CR1-KO mice in ELISPOT assays performed at 11 and 60 d p.i. The results show that during disease initiation IFN-γ Ag-specific producing T cells were detected in higher frequency in lymph node tissues (Fig. 3A). IL-17–producing T cells were significantly abundant in both lymph nodes (Fig. 3A) and spleen tissues of CX3CR1-KO mice (Fig. 3B) when compared with WT mice at 11 d p.i. By day 60 p.i., the frequency of Ag-specific T cells producing IFN-γ or IL-17 was undetectable in lymph nodes (data not shown). However, in the spleen, both WT and KO mice revealed IFN-γ–producing cells in comparable frequencies. In addition, the frequency of IL-17–producing T cells was higher in CX3CR1-deficient mice when compared with WT mice, with a notable decrease at 60 d p.i. (Fig. 3B). The results suggest that CX3CR1-KO mice exhibited increased numbers of peripheral IL-17–secreting Ag-specific T cells. Due to the differential inflammatory response visualized

Downloaded from http://www.jimmunol.org/jimmunol/article-pdf/191/3/1063/1379268/1300040.pdf by guest on 19 April 2024

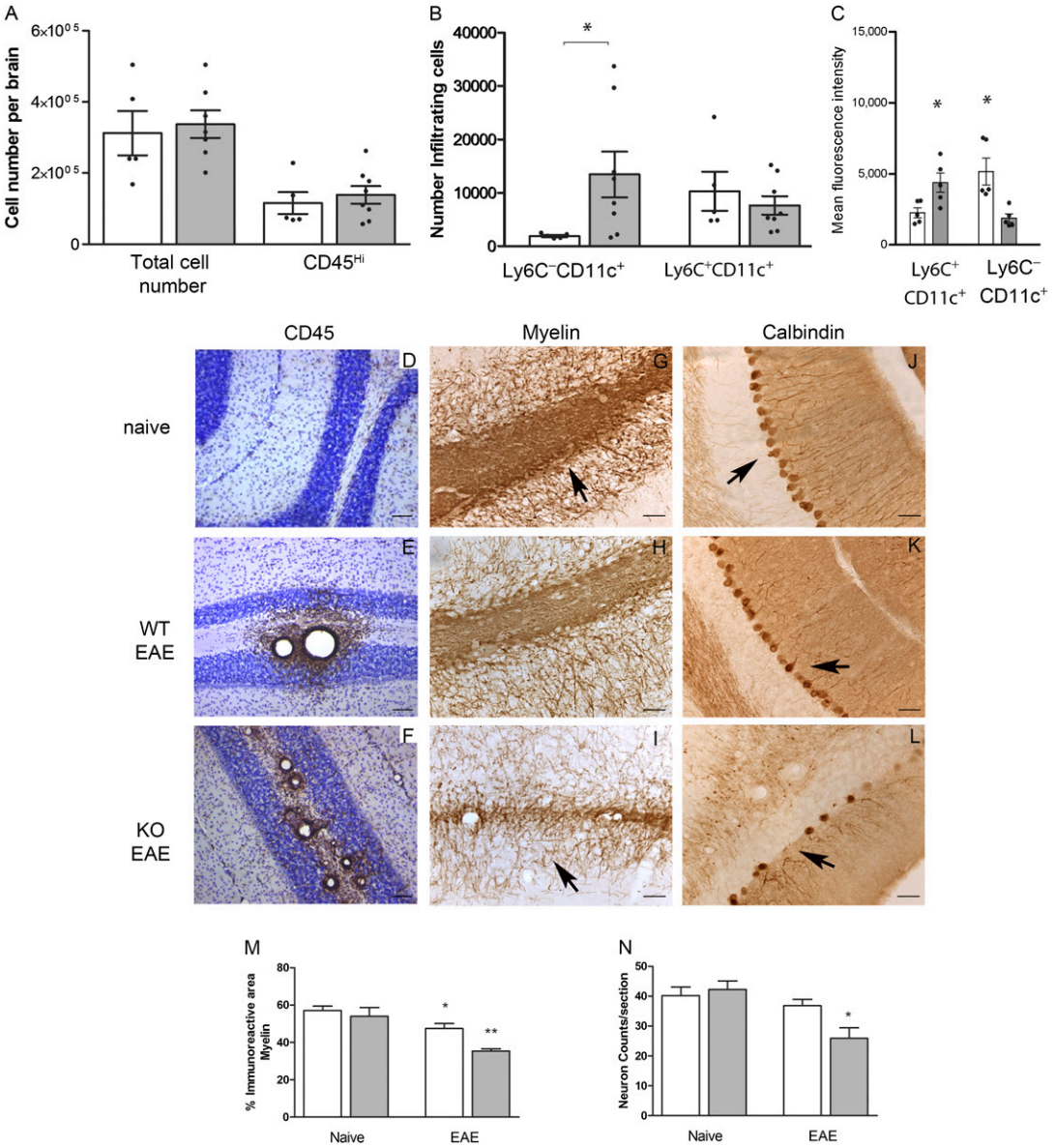

FIGURE 2. CX3CR1-deficient mice showed an increased accumulation of CD11c$^+$ dendritic cells in CNS correlating with more severe CNS pathology. Brain mononuclear cells isolated at peak of EAE disease from *Cx3cr1*$^{+/GFP}$/*Ccr2*$^{+/RFP}$ and *Cx3cr1*$^{GFP/GFP}$/*Ccr2*$^{+/RFP}$ were separated over Percoll gradients and analyzed by flow cytometry. (**A**) Total number of brain mononuclear cells and CD45^{high} infiltrating cells. (**B**) CD45^{high} infiltrating cells were gated to quantify myeloid cell subsets based on expression of CD115, Ly6C, and CD11c. Open bars, *Cx3cr1*$^{+/GFP}$/*Ccr2*$^{+/RFP}$ mice with normal receptor function; gray bars, CX3CR1-deficient *Cx3cr1*$^{GFP/GFP}$/*Ccr2*$^{+/RFP}$ mice (*$p < 0.05$). (**C**) CX3CR1-GFP (open bars) and CCR2-RFP (gray bars) fluorescence intensities in monocyte subsets were compared in *Cx3cr1*$^{+/GFP}$/*Ccr2*$^{+/RFP}$ mice (*$p < 0.05$). Values are mean ± SEM. Results are representative of two similar experiments. Brain tissues were stained with anti-CD45 Abs (brown staining) as a marker of global inflammation and counterstained with Nissl (**D**–**F**), anti-MBP Abs to assess demyelination (**G**–**I**), and anti-calbindin Abs to visualize cerebellar Purkinje cells (**J**–**L**) in *Cx3cr1*$^{-/-}$ naive (D, G, J), diseased WT (E, H, K), and *Cx3cr1*$^{-/-}$ (F, I, and L) mice. Scale bars (D–F), 100 μm (original magnification ×10); (G–L), 50 μm original magnification ×20). (**M**) Myelin immunoreactive area, *$p = 0.03$ between WT naive and WT-EAE groups, **$p < 0.0001$ between WT-EAE and KO-EAE groups. (**N**) Calbindin-positive cells per section were counted in four mice per group, *$p = 0.04$ between WT-EAE and KO-EAE groups. Open bars represent WT mice, and gray bars represent the KO group.

by tissue immunohistochemistry, cytokine expression was also assessed in the CNS by quantitative RT-PCR and analyzed separately in forebrain, cerebellum, and spinal cord regions. Compared with WT mice, CX3CR1-KO mice exhibited increased mRNA transcript expression of IFN-γ in cerebellar and spinal cord tissues (Fig. 3C), and increase in IL-17 was revealed in forebrain and cerebellar regions (Fig. 3D, *$p = 0.005$). The anti-inflammatory cytokine IL-10 was detected at significantly higher levels in spinal cord tissues of WT mice (Supplemental Fig. 3A, **$p = 0.0008$), whereas in all CNS tissues of CX3CR1-deficient mice, TNF-α levels were higher when compared with diseased WT mice (Supplemental Fig. 3B). Cytokine ELISPOT assays (Fig. 3E) using total brain leukocyte populations at peak of EAE disease revealed a significant increase in the number of IL-17–producing cells from CX3CR1-KO mice and a higher ratio of IL-17/IFN-γ spot-forming cells when compared with WT mice (Fig. 3F, *$p <$ 0.05). Overall, our results suggest an important role for CX3CR1/CX3CL1 in the regulation of APC effector function and in turn in the modulation of the development of a proinflammatory environment.

Downloaded from http://www.jimmunol.org/jimmunol/article-pdf/191/3/1063/1379268/1300040.pdf by guest on 19 April 2024

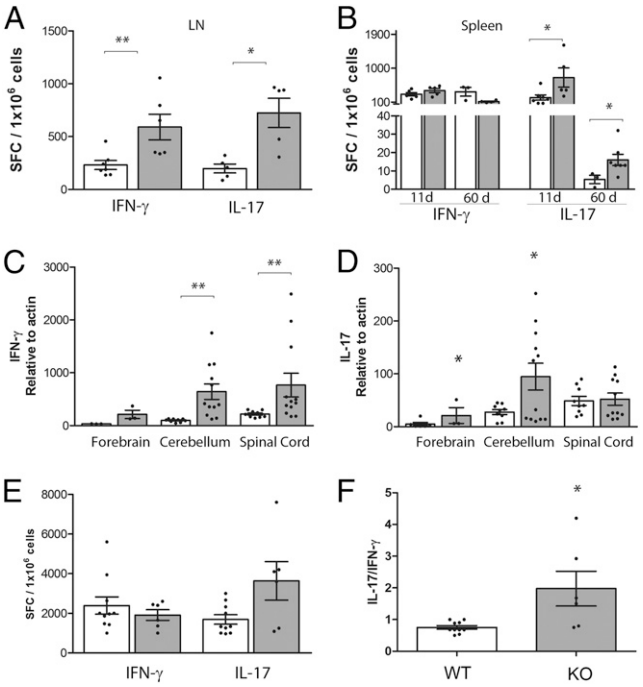

FIGURE 3. Cytokine expression in peripheral and CNS tissues. Lymph nodes (**A**) and spleen cell suspensions (**B**) were subjected to IFN-γ and IL-17 ELISPOT assays. Cytokine expression was measured at peak of EAE disease in brain, spinal cord (SC), and cerebellar (Cer) tissues of WT (open bars) and *Cx3cr1*$^{-/-}$ mice (gray bars) using quantitative RT-PCR in TaqMan assays for IFN-γ (**C**) and IL-17 (**D**). ELISPOT assays (**E**) and the ratio of IL-17/IFN-γ from the same sample are shown in (**F**). Dots on graph represent sample from an individual mouse. *$p < 0.05$, **$p < 0.01$.

Effect of CX3CR1 deficiency on APC effector function

To address the role of CX3CR1 on dendritic cells and their effects to modulate T cell function, we performed in vitro proliferation assays using $MOG_{35–55}$-primed T cells isolated from actively immunized WT mice at day 11 p.i. T cells were then mixed with WT or *Cx3cr1*$^{-/-}$ APCs ($CD11b^+CD11c^+$) isolated from spleens and lymph nodes or from diseased brains and dilution of the proliferation dye on T cells evaluated. Cultured cells were stained with the viability dye eFluor780 (Fig. 4A), and only live $CD4^+$ T cells were analyzed (Fig. 4B). Cultures containing WT dendritic cells (Fig. 4C, 4D) revealed less proliferating T cells when compared with cultures containing CX3CR1-KO peripheral dendritic cells (Fig. 4C, 4D). A similar result was obtained when using CNS-derived myeloid cells (Supplemental Fig. 4). To further address the role of CX3CR1 on adaptive immunity via modulation of myeloid cell function, we examined expression of class II histocompatibility Ags $I\text{-}A^b$ and the costimulatory molecules CD80 and CD86 in spleen and lymph node myeloid cells (Fig. 5A, 5C) from actively immunized mice at 11 d p.i. and from brain leukocyte populations at peak of EAE disease (Fig. 5B, 5D). The proportions of myeloid subsets $CD11b^+Ly6C^+CD11c^+$ and $CD11b^+Ly6C^-CD11c^+$ in spleen and lymph nodes of actively immunized mice were comparable between WT and CX3CR1-KO mice. However, CX3CR1-KO cells exhibited increased surface expression of MHC-II (Fig. 5A, *$p = 0.03$). Similarly, $CD11c^+$ cells isolated from inflamed CX3CR1-KO brains showed increased surface expression of MHC-II and CD86 when compared with WT mice. Notably, in the brain the $CD45^{high}CD11c^+$ population predominates in MHC-II expression when compared with the $CD45^{low}CD11b^+$ microglia population or with the infiltrating myeloid cell population that is CD11c negative (Fig. 5B, *$p <$ 0.05). Interestingly, CD86 expression was found upregulated in all CX3CR1-KO myeloid populations not only in lymphoid tissues (Fig. 5C), but also in the brain, including microglia, and infiltrating $CD11b^+CD11c^-$ and $CD11b^+CD11c^+$ populations (Fig. 5D, *$p < 0.05$).

To assess differences in the proliferation of the CNS myeloid cells, we performed flow cytometry on cells isolated from diseased WT (Fig. 6A, 6B) and KO (Fig. 6C, 6D) brains. The cells were stained with Abs against CD45, CD11c, CD11b, and the proliferation marker Ki67. CX3CR1-KO mice exhibited a higher proportion of $Ki67^+$ myeloid cells that included the $CD45^{low}CD11b^+$ microglia and $CD45^{high}CD11b^+CD11c^+$ infiltrating dendritic cells (Fig. 6C). Altogether, the results indicate that CX3CR1 plays an important role in modulating the activation of peripheral and CNS APCs.

CX3CR1 modulates EAE severity via regulation of APC function

To strengthen the previous results, we investigated the role of CX3CR1 on the effector phase of EAE by comparing disease course after adoptive transfer of WT T cells or KO T cells in WT and KO recipients (Fig. 7). Given the fact that the frequencies of IFN-γ– and IL-17–producing T cells was higher (almost 3×-fold) in KO mice upon induction of EAE via active immunization, donor T cells for adoptive transfer experiments were analyzed by ELISPOT assays for IFN-γ and IL-17 to determine the overall numbers of effector cells elicited. The numbers of cells to be injected for the adoptive transfer experiments were adjusted to reflect similar proportions of IFN-γ– and IL-17–producing cells in both donor WT and KO T cells. The data indicated that $MOG_{35–55}$-primed *Cx3cr1*$^{-/-}$ (Fig. 7A, 7B) or *Cx3cr1*$^{+/+}$ T cells (Fig. 7A, 7C, 7D) induced a similar EAE phenotype as shown by the maximum EAE score in the four experimental groups analyzed. From four different experiments analyzed, the incidence of EAE was higher in the KO recipients with ~80% of mice displaying neurologic signs. EAE manifestations were more severe in *Cx3cr1*$^{-/-}$ recipient regardless of the genotype of the T cells used for the passive transfer of EAE.

Discussion

The diversity and polarization capacity of the myeloid cells, including microglia, monocytes, macrophages, and dendritic cells, have introduced a challenge to understand the function of the myeloid lineage during conditions that involve microbial pathogens, autoimmune inflammation, or neurodegeneration (29). In general, the mononuclear phagocyte system plays an important role in development, scavenging, inflammation, and antimicrobial defenses. However, cell signaling pathways elicited in response to extracellular signals guide the development of distinct population of myeloid cells (30). Main subsets of blood monocytes that have been studied in mice can be distinguished on the basis of Ly6C/CCR2/CX3CR1 expression. Inflammatory $Ly6C^+/CCR2^{high}/CX3CR1^{low}$ murine monocytes are believed to be recruited from blood to tissues following infection, where they undergo activation and their response appears to be pathogen dependent. In contrast, $Ly6C^-/CCR2^{low}/CX3CR1^{high}$ monocytes appear to populate normal tissues and exhibit long-range crawling over the endothelium of capillaries, small veins, and arteries, a process that may be involved in surveillance. $Ly6C^-$ monocytes are suggested to be involved in tissue repair, but a role in regulating T cell function is not yet described. It has also been defined that a fraction of murine monocytes exhibits suppressor functions and can be found in the spleen or liver of mice and inhibits T cell proliferation. In humans, $CD14^+$ monocytes that consist of $CD16^+$ and $CD16^-$ cells re-

Downloaded from http://www.jimmunol.org/jimmunol/article-pdf/191/3/1063/1379268/1300040.pdf by guest on 19 April 2024

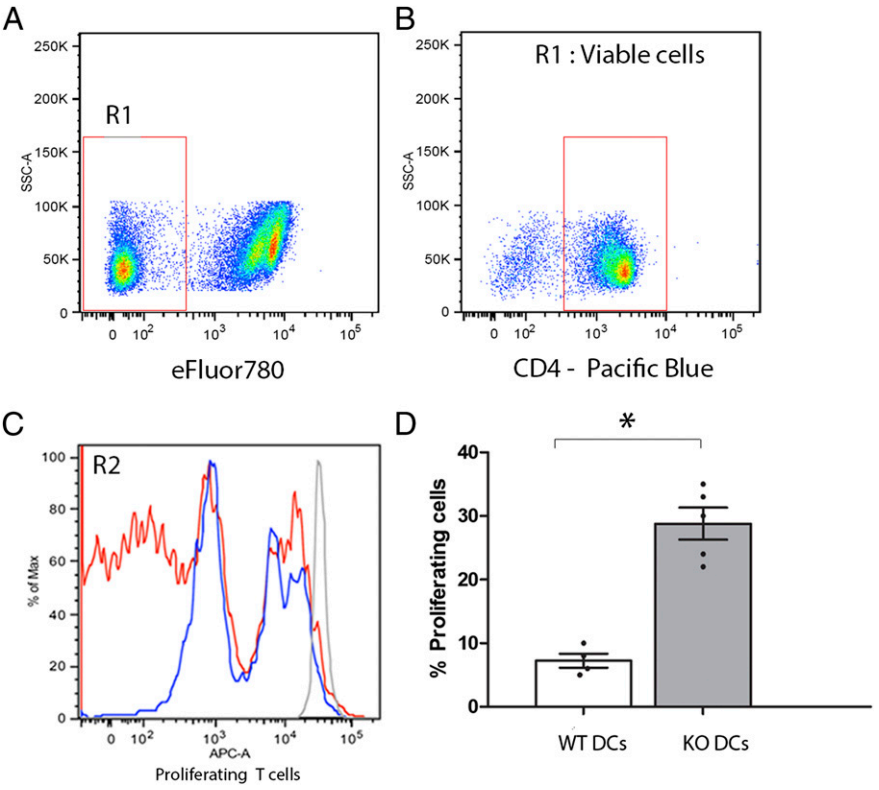

FIGURE 4. Effect of CX3CR1 on APCs for T cell proliferation. $MOG_{35–55}$-primed T cells were enriched from WT mice 11 d p.i., labeled with CFSE, and incubated with $CD11b^+$ $CD11c^+$ dendritic cells isolated from WT or *Cx3cr1*$^{-/-}$ mice in presence of 20 μg/ml $MOG_{35–55}$ Ag. Proliferation was assessed by flow cytometry on live (**A**) and $CD4^+$ T cells (**B**). A representative experiment is shown using primed WT T cells cultured with WT (**C**, blue line) or *Cx3cr1*$^{-/-}$ (C, red line) dendritic cells and compared in overlapping histograms (C); faint gray line represents the positive control. Data are presented as percentage of WT T cell proliferation in three to five different experiments in the presence of WT (**D**, open bar) or CX3CR1-KO dendritic cells (D, gray bar), $*p < 0.05$.

semble $Ly6C^+$ murine monocytes. In contrast, murine patrolling $Ly6C^-$ monocytes are more similar to the human $CD14^{low}$ subset (13). Although the heterogeneity of monocytes is complex, current data support the notion that $Ly6C^+/CCR2^{high}/CX3CR1^{low}$ and $Ly6C^-/CCR2^{low}/CX3CR1^{high}$ commit to differentiate more readily into M1-like and M2-like inflammatory monocytes or dendritic cells, respectively (30).

The fractalkine receptor, CX3CR1, plays neuroprotective roles in selected CNS pathologies, including the CX3CR1-SOD^{G93A} transgenic mouse model of amyotrophic lateral sclerosis. Also, the absence of CX3CR1 led to increased levels of IL-1β and enhanced neuronal damage after peripheral LPS administration in a model of low-level endotoxemia (2). In addition, CX3CR1-deficient mice exhibited an increased loss of tyrosine-hydroxylase–positive neurons in the substantia nigra pars compacta after acute 1-methy1-4-pheny1-1,2,3,6-tetrahydropyridine (MPTP) intoxication, which correlated with robust microglial activation. However, no effect on striatal dopaminergic contenta was observed when *Cx3cr1*$^{-/-}$ mice were treated with methamphetamine (31). Also during EAE, CX3CR1 appears to be protective (28) by affecting

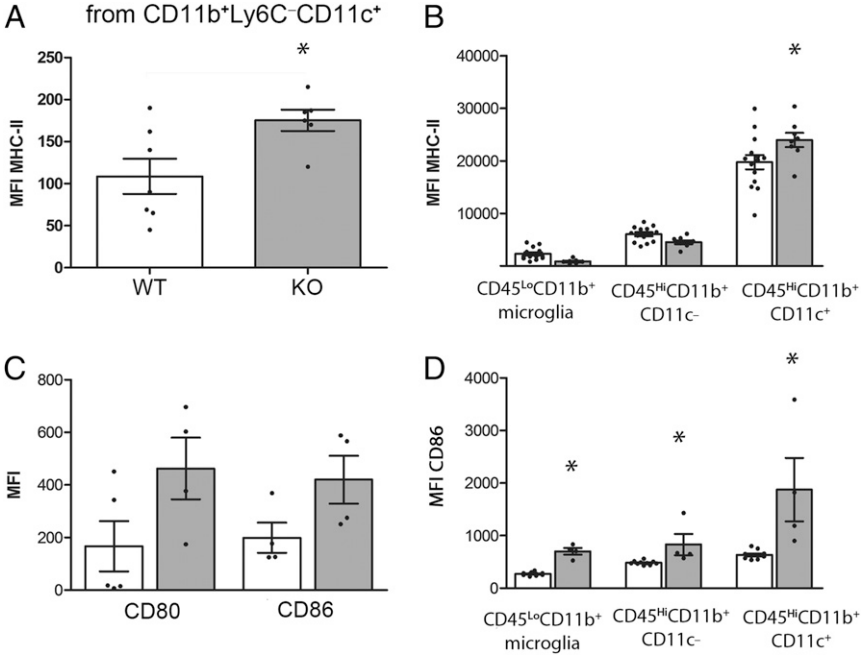

FIGURE 5. Effect of CX3CR1 deficiency on APC-related molecules. Lymph nodes and brain mononuclear cells were isolated at 11 d p.i. and at peak of EAE disease, respectively, and analyzed for the myeloid subsets CD45, CD11b, Ly6C, and CD11c by flow cytometry. Mean fluorescence intensity for MHC-II in lymph node (**A**) and brain leukocytes (**B**) and CD80 and CD86 (**C**, **D**) was compared between WT (open bars) and KO mice (gray bars). Each dot represents data from pooled inguinal lymph nodes from one mouse and from one brain at peak EAE disease. $*p < 0.05$.

Downloaded from http://www.jimmunol.org/jimmunol/article-pdf/191/3/1063/1379268/1300040.pdf by guest on 19 April 2024

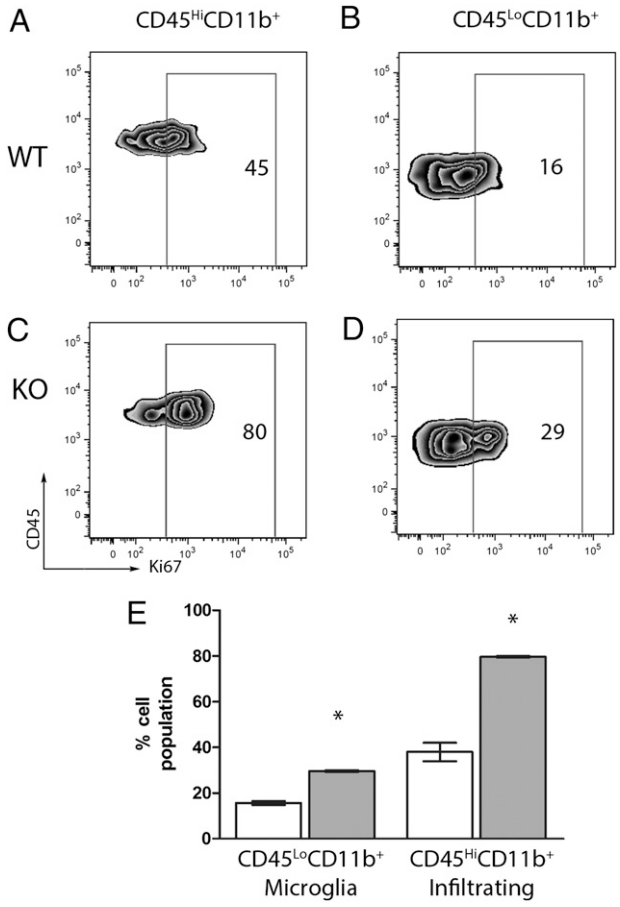

FIGURE 6. CX3CR1-deficient myeloid cells proliferate more readily in the CNS. Brain mononuclear cells were compared in WT (**A**, **B**) and KO mice (**C**, **D**). The proportion of proliferating Ki67$^+$ cells (**E**) was then assessed on the gated population based on the expression of CD45 and CD11b, as CD45^{high}CD11b$^+$ (A, C) and CD45^{low}CD11b$^+$ (B, D) in WT (open bars) and KO (gray bars) mice. *$p < 0.05$.

the accumulation of NK cells to CNS tissues, but the role of CX3CR1 in myeloid cell trafficking and function has not been addressed. Fractalkine, the sole CX3CR1 ligand, displays properties of both chemokines and adhesion molecules, acting as a chemoattractant for cells expressing the receptor and mediating high-affinity adhesion when membrane-tethered fractalkine interacts with CX3CR1$^+$ monocytes. The neuroprotective function of CX3CL1 was first reported in hippocampal neurons via CX3CR1 blockade in vitro (32). In an excitotoxic model of neuronal death, CX3CL1 promoted survival of hippocampal neurons and CX3CL1-mediated microglial release of adenosine contributed to neuronal protection via upregulation of neuronal adenosine receptor AR1 (33, 34). Conversely, CX3CR1 blockade was associated with smaller infarct size and enhanced recovery in a model of focal cerebral ischemia (35). From these studies, blocking CX3CL1 signaling seemed to be deleterious during CNS inflammation.

We have identified an important role of CX3CR1 for APC effector function in mouse models of MS. CX3CR1-expressing mice exhibit Ly6C^{high}CX3CR1^{low} monocytes that control the inflammatory lesions (19), whereas, in absence of CX3CR1, the inflammatory reaction in the CNS is dominated by a population of dendritic cells that is CD11b$^+$Ly6C$^-$CD11c$^+$CX3CR1^{high}. Therefore, CX3CR1-deficient mice provide a novel model to further characterize these cells under various chronic inflammatory settings. This population showed increased expression of markers of Ag presentation and costimulation and induced T cell proliferation, and the affected CNS correlated with a predominance of IL-17–producing cells (Fig. 3D, 3F). The mechanism linking CX3CL1/CX3CR1 interaction to modulation of Ag presentation and costimulation is under current investigation. The involvement of fractalkine signaling and regulation of the master MHC-II regulator CIITA is a likely target as well as several STAT molecules. We have evidence that myeloid cells from CX3CL1 (ligand)-deficient mice upon LPS stimulation exhibit upregulation of MHC-II, and addition of recombinant mouse fractalkine decreased MHC-II expression on both CD11c$^+$ and CD11c$^-$ myeloid cell populations (J.A. Garcia, S.M. Cardona, S. Adkins, and A.E. Cardona, unpublished observations). Therefore, defining the players in this signaling pathway is the next step to further our understanding of the neuroprotective effects of fractalkine during autoimmune inflammation.

Overall, the findings of our studies are of great relevance due to the implication of the human polymorphic variants (V249I and T280M) in altering fractalkine-receptor binding affinity (12) as well as expression level of CX3CR1 (9). The association of the variant receptor with chronic inflammatory diseases, including Crohn's disease (36), atherosclerosis, and coronary artery disease (10, 12, 37), has been demonstrated. Importantly, protective roles in atherosclerosis and acute coronary events have been suggested (38, 39), contrasting an association to increased susceptibility to age-reacted macular degeneration. The decreased binding of the variant receptors to the ligand CX3CL1 on peripheral endothelial cells may explain the protective effects in settings of peripheral inflammation. However, little is known about the association of human CX3CR1 variants in CNS conditions. From our data in experimental mice with defective CX3CR1 signaling, we argue that abnormal CX3CR1–CX3CL1 interactions will be deleterious due to increased influx of highly activated myeloid populations that might potentially enhance and sustain T cell responses within the CNS. A genetic analysis of MS patients revealed significantly lower frequency of the CX3CR1$^{I249/T280}$ haplotype in secondary progressive patients when compared with relapsing–remitting patients (40). Therefore, there is a possible protective effect of the reference I249 allele on secondary-progressive MS when linked with T280. Findings in MS patients added to our results show that CX3CR1 deficiency alters not only the NK cell compartment, but also myeloid cell lineage and potentially microglial cells, and additional human studies should be directed to identify possible associations of these polymorphic variants with CNS inflammation. The results presented showed that absence of CX3CR1 correlated with enhanced brain inflammation and more severe EAE neurologic signs. Reconstitution of WT recipients with CX3CR1-deficient bone marrow revealed that peripheral CX3CR1 has a profound effect in CNS inflammation, as a more severe neurologic disease developed in these mice. The pathology in the CX3CR1-deficient mice showed that the inflammatory reaction correlated with more demyelination and neuronal damage. To further investigate mechanisms that lead to differences in myelin density between WT and CX3CR1-deficient mice, we compared Olig2 and ciliary neurotrophic factor (CNTF) expression by immunohistochemistry in brain sections from WT and KO mice at peak disease (our unpublished data). Olig2$^+$ cells appear increased in cerebellar areas of EAE-affected CX3CR1-KO mice when compared with WT mice. Expression of CNTF was abundant in cerebellar regions of naive and EAE WT mice, but was reduced in diseased KO mice. Therefore, we hypothesize that CX3CR1-KO mice exhibit a defect in demyelination. How the inflammatory reaction contributes to modulation of CNTF expression is still under investigation.

Downloaded from http://www.jimmunol.org/jimmunol/article-pdf/191/3/1063/1379268/1300040.pdf by guest on 19 April 2024

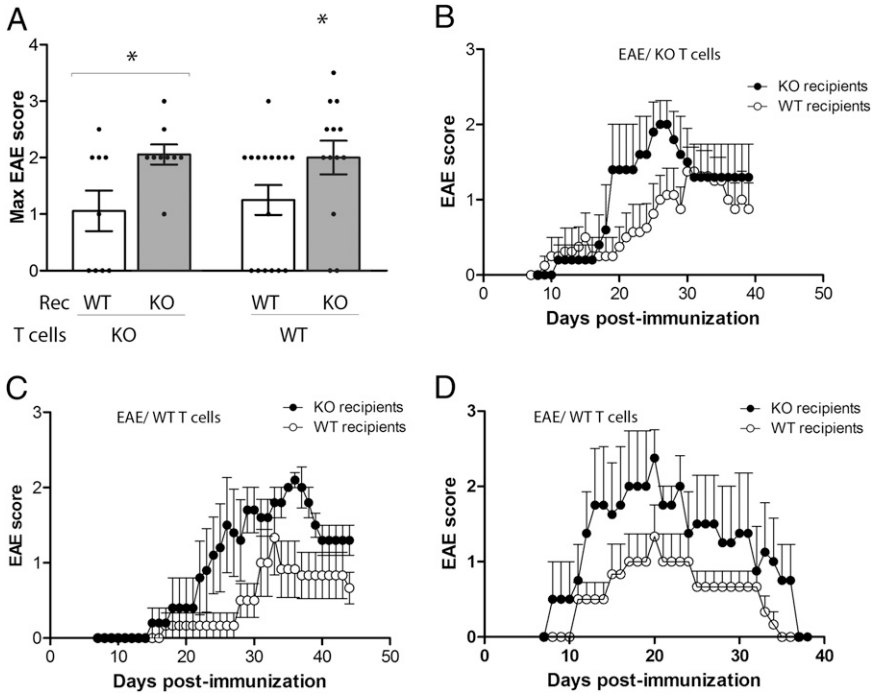

FIGURE 7. EAE signs were more severe in *Cx3cr1*$^{-/-}$ recipient regardless of the genotype of the T cells used for the passive transfer of EAE. Cells for adoptive transfer EAE were prepared from WT and CX3CR1-deficient mice and disease compared in WT or KO recipient mice (Rec). EAE maximum scores (**A**) and disease progression were monitored daily in recipients of primed KO T cells (**B**); two (**C**, **D**) of three separate experiments of recipients of WT T cells are shown. Dots in (A) represent an individual mouse. $*p < 0.05$.

Comparison of myeloid cell subsets showed an enrichment of monocyte-derived (CD115$^+$) Ly6C$^-$CD11c$^+$ dendritic cells in the EAE brain. Although Ly6C$^-$ monocytes migrate to CNS under steady-state conditions, they do not tend to home to sites of inflammation. However, our data showed that, in absence of CX3CR1 signaling, this particular Ly6C$^-$CD11c$^+$ subset more readily infiltrates the inflamed brain, where it undergoes proliferation and may play an important role in sustaining encephalitogenic T cell responses. We focused our studies on investigating the role of CX3CR1 for APC function, including modulation of costimulatory molecules and MHC-II presentation, and found that CX3CR1-deficient APCs showed a higher expression of molecules involved in T cell costimulation. In humans, immunosenescence has been associated with the peripheral expansion of a population of CD4$^+$CD28$^-$ T cells. In MS patients, this particular subset exhibited a cytotoxic phenotype and CX3CR1 discriminated these cells from their CD4$^+$CD28$^+$ counterparts. Importantly, CD4$^+$CD28$^+$ T cells accumulate in MS lesions of a subgroup of patients, but their exact contribution of CX3CR1 in the modulation of the cytotoxic phenotype is uncertain (41). The role of CX3CR1 on murine T cells has not been explored, as only a small percentage of peripheral T cells expresses CX3CR1. We are currently addressing inflammatory conditions that may trigger upregulation of CX3CR1 on T cells and that could subsequently alter effector immune responses. In the current study, to address the role of CX3CR1 on T cells, we compared adoptive transferred EAE in KO and WT recipients using primed WT or KO T cells. It is important to note that *Cx3cr1*$^{-/-}$ mice elicited a higher frequency of IL-17–producing cells, but we addressed this issue by injecting similar numbers of IL-17–producing cells. Therefore, EAE disease was compared in adoptive transfer settings using equivalent number of encephalitogenic T cells from primed WT or *Cx3cr1*$^{-/-}$ mice. Altogether, the adoptive transfer EAE results suggest that CX3CR1 deficiency on T cells does not affect disease severity.

From the cytokine analysis, elevated levels of TNF-α in brain and spinal cord of CX3CR1-KO mice produced by the abundant myeloid population and/or T cells may contribute to the maintenance of the inflammatory reaction within the CNS, as previously shown. During EAE, TNF has been shown to produce contrasting pathogenic and protective roles in CNS and secondary lymphoid organs, respectively. In the CNS, TNF on myeloid cells has been shown to accelerate onset of EAE by regulating chemokine expression (42) and driving recruitment of inflammatory cells to the CNS by acting on the endothelium of the blood brain barrier (43). TNF can also function by activating microglia and astrocytes (44, 45) and promoting upregulation of adhesion molecules (46, 47).

Our data support the notion that CX3CR1 plays neuroprotective roles during EAE and suggest that peripheral CX3CR1 expression restricts trafficking of Ly6C^{low}CX3CR1^{high} cells to the CNS most likely by interaction with the peripherally expressed ligand. As we advance our knowledge in the understanding of myeloid cell subtypes, it is important to clarify whether they arise from a common bone marrow precursor or whether they differentiate within particular tissues under the pressures of the surrounding environment to exert specialized functions. CX3CR1, as an inflammatory and regulatory receptor, poses an intriguing biology, and its role in the human population under various neuroinflammatory conditions is yet to be determined.

Acknowledgments

We thank Difernando Vanegas (University of Texas Health Science Center at San Antonio) for assistance in the generation of the bone marrow chimeras, Niannian Ji (University of Texas at San Antonio) for technical assistance with the ELISPOT assay, the Research Centers in Minority Institutions Advanced Imaging Center (University of Texas at San Antonio), and Elizabeth Morris (University of Texas at San Antonio) for secretarial assistance.

Disclosures

The authors have no financial conflicts of interest.

References

1. Cardona, A. E., M. E. Sasse, L. Liu, S. M. Cardona, M. Mizutani, C. Savarin, T. Hu, and R. M. Ransohoff. 2008. Scavenging roles of chemokine receptors: chemokine receptor deficiency is associated with increased levels of ligand in circulation and tissues. *Blood* 112: 256–263.

Downloaded from http://www.jimmunol.org/jimmunol/article-pdf/191/3/1063/1379268/1300040.pdf by guest on 19 April 2024

2. Cardona, A. E., E. P. Pioro, M. E. Sasse, V. Kostenko, S. M. Cardona, I. M. Dijkstra, D. Huang, G. Kidd, S. Dombrowski, R. Dutta, et al. 2006. Control of microglial neurotoxicity by the fractalkine receptor. *Nat. Neurosci.* 9: 917–924.
3. Bazan, J. F., K. B. Bacon, G. Hardiman, W. Wang, K. Soo, D. Rossi, D. R. Greaves, A. Zlotnik, and T. J. Schall. 1997. A new class of membrane-bound chemokine with a CX3C motif. *Nature* 385: 640–644.
4. Rossi, D. L., G. Hardiman, N. G. Copeland, D. J. Gilbert, N. Jenkins, A. Zlotnik, and J. F. Bazan. 1998. Cloning and characterization of a new type of mouse chemokine. *Genomics* 47: 163–170.
5. Combadiere, C., K. Salzwedel, E. D. Smith, H. L. Tiffany, E. A. Berger, and P. M. Murphy. 1998. Identification of CX3CR1: a chemotactic receptor for the human CX3C chemokine fractalkine and a fusion coreceptor for HIV-1. *J. Biol. Chem.* 273: 23799–23804.
6. Mizoue, L. S., J. F. Bazan, E. C. Johnson, and T. M. Handel. 1999. Solution structure and dynamics of the CX3C chemokine domain of fractalkine and its interaction with an N-terminal fragment of CX3CR1. *Biochemistry* 38: 1402–1414.
7. Hatori, K., A. Nagai, R. Heisel, J. K. Ryu, and S. U. Kim. 2002. Fractalkine and fractalkine receptors in human neurons and glial cells. *J. Neurosci. Res.* 69: 418–426.
8. Tuo, J., B. C. Smith, C. M. Bojanowski, A. D. Meleth, I. Gery, K. G. Csaky, E. Y. Chew, and C. C. Chan. 2004. The involvement of sequence variation and expression of CX3CR1 in the pathogenesis of age-related macular degeneration. *FASEB J.* 18: 1297–1299.
9. Chan, C. C., J. Tuo, C. M. Bojanowski, K. G. Csaky, and W. R. Green. 2005. Detection of CX3CR1 single nucleotide polymorphism and expression on archived eyes with age-related macular degeneration. *Histol. Histopathol.* 20: 857–863.
10. Moatti, D., S. Faure, F. Fumeron, Mel.-W. Amara, P. Seknadji, D. H. McDermott, P. Debré, M. C. Aumont, P. M. Murphy, D. de Prost, and C. Combadière. 2001. Polymorphism in the fractalkine receptor CX3CR1 as a genetic risk factor for coronary artery disease. *Blood* 97: 1925–1928.
11. Nassar, B. A., A. A. Nanji, T. P. Ransom, K. Rockwood, S. A. Kirkland, K. Macpherson, P. W. Connelly, D. E. Johnstone, B. J. O'Neill, I. R. Bata, et al. 2008. Role of the fractalkine receptor CX3CR1 polymorphisms V249I and T280M as risk factors for early-onset coronary artery disease in patients with no classic risk factors. *Scand. J. Clin. Lab. Invest.* 68: 286–291.
12. McDermott, D. H., A. M. Fong, Q. Yang, J. M. Sechler, L. A. Cupples, M. N. Merrell, P. W. Wilson, R. B. D'Agostino, C. J. O'Donnell, D. D. Patel, and P. M. Murphy. 2003. Chemokine receptor mutant CX3CR1-M280 has impaired adhesive function and correlates with protection from cardiovascular disease in humans. *J. Clin. Invest.* 111: 1241–1250.
13. Auffray, C., D. Fogg, M. Garfa, G. Elain, O. Join-Lambert, S. Kayal, S. Sarnacki, A. Cumano, G. Lauvau, and F. Geissmann. 2007. Monitoring of blood vessels and tissues by a population of monocytes with patrolling behavior. *Science* 317: 666–670.
14. Geissmann, F., S. Jung, and D. R. Littman. 2003. Blood monocytes consist of two principal subsets with distinct migratory properties. *Immunity* 19: 71–82.
15. Geissmann, F., S. Gordon, D. A. Hume, A. M. Mowat, and G. J. Randolph. 2010. Unravelling mononuclear phagocyte heterogeneity. *Nat. Rev. Immunol.* 10: 453–460.
16. Auffray, C., M. H. Sieweke, and F. Geissmann. 2009. Blood monocytes: development, heterogeneity, and relationship with dendritic cells. *Annu. Rev. Immunol.* 27: 669–692.
17. Geissmann, F., C. Auffray, R. Palframan, C. Wirrig, A. Ciocca, L. Campisi, E. Narni-Mancinelli, and G. Lauvau. 2008. Blood monocytes: distinct subsets, how they relate to dendritic cells, and their possible roles in the regulation of T-cell responses. *Immunol. Cell Biol.* 86: 398–408.
18. Mizutani, M., P. A. Pino, N. Saederup, I. F. Charo, R. M. Ransohoff, and A. E. Cardona. 2012. The fractalkine receptor but not CCR2 is present on microglia from embryonic development throughout adulthood. *J. Immunol.* 188: 29–36.
19. Saederup, N., A. E. Cardona, K. Croft, M. Mizutani, A. C. Cotleur, C. L. Tsou, R. M. Ransohoff, and I. F. Charo. 2010. Selective chemokine receptor usage by central nervous system myeloid cells in CCR2-red fluorescent protein knock-in mice. *PLoS One* 5: e13693.
20. Bettelli, E., Y. Carrier, W. Gao, T. Korn, T. B. Strom, M. Oukka, H. L. Weiner, and V. K. Kuchroo. 2006. Reciprocal developmental pathways for the generation of pathogenic effector TH17 and regulatory T cells. *Nature* 441: 235–238.
21. Yang, Y., J. Weiner, Y. Liu, A. J. Smith, D. J. Huss, R. Winger, H. Peng, P. D. Cravens, M. K. Racke, and A. E. Lovett-Racke. 2009. T-bet is essential for encephalitogenicity of both Th1 and Th17 cells. *J. Exp. Med.* 206: 1549–1564.
22. Thakker, P., M. W. Leach, W. Kuang, S. E. Benoit, J. P. Leonard, and S. Marusic. 2007. IL-23 is critical in the induction but not in the effector phase of experimental autoimmune encephalomyelitis. *J. Immunol.* 178: 2589–2598.
23. Pino, P. A., and A. E. Cardona. 2011. Isolation of brain and spinal cord mononuclear cells using Percoll gradients. *J. Vis. Exp.* 48: e2348.
24. Haskell, C. A., W. W. Hancock, D. J. Salant, W. Gao, V. Csizmadia, W. Peters, K. Faia, O. Fituri, J. B. Rottman, and I. F. Charo. 2001. Targeted deletion of CX (3)CR1 reveals a role for fractalkine in cardiac allograft rejection. *J. Clin. Invest.* 108: 679–688.
25. Jung, S., J. Aliberti, P. Graemmel, M. J. Sunshine, G. W. Kreutzberg, A. Sher, and D. R. Littman. 2000. Analysis of fractalkine receptor CX(3)CR1 function by targeted deletion and green fluorescent protein reporter gene insertion. *Mol. Cell. Biol.* 20: 4106–4114.
26. Haskell, C. A., M. D. Cleary, and I. F. Charo. 2000. Unique role of the chemokine domain of fractalkine in cell capture: kinetics of receptor dissociation correlate with cell adhesion. *J. Biol. Chem.* 275: 34183–34189.
27. Haskell, C. A., M. D. Cleary, and I. F. Charo. 1999. Molecular uncoupling of fractalkine-mediated cell adhesion and signal transduction: rapid flow arrest of CX3CR1-expressing cells is independent of G-protein activation. *J. Biol. Chem.* 274: 10053–10058.
28. Huang, D., F. D. Shi, S. Jung, G. C. Pien, J. Wang, T. P. Salazar-Mather, T. T. He, J. T. Weaver, H. G. Ljunggren, C. A. Biron, et al. 2006. The neuronal chemokine CX3CL1/fractalkine selectively recruits NK cells that modify experimental autoimmune encephalomyelitis within the central nervous system. *FASEB J.* 20: 896–905.
29. Prinz, M., J. Priller, S. S. Sisodia, and R. M. Ransohoff. 2011. Heterogeneity of CNS myeloid cells and their roles in neurodegeneration. *Nat. Neurosci.* 14: 1227–1235.
30. Geissmann, F., M. G. Manz, S. Jung, M. H. Sieweke, M. Merad, and K. Ley. 2010. Development of monocytes, macrophages, and dendritic cells. *Science* 327: 656–661.
31. Thomas, D. M., D. M. Francescutti-Verbeem, and D. M. Kuhn. 2008. Methamphetamine-induced neurotoxicity and microglial activation are not mediated by fractalkine receptor signaling. *J. Neurochem.* 106: 696–705.
32. Meucci, O., A. Fatatis, A. A. Simen, and R. J. Miller. 2000. Expression of CX3CR1 chemokine receptors on neurons and their role in neuronal survival. *Proc. Natl. Acad. Sci. USA* 97: 8075–8080.
33. Lauro, C., S. Di Angelantonio, R. Cipriani, F. Sobrero, L. Antonilli, V. Brusadin, D. Ragozzino, and C. Limatola. 2008. Activity of adenosine receptors type 1 is required for CX3CL1-mediated neuroprotection and neuromodulation in hippocampal neurons. *J. Immunol.* 180: 7590–7596.
34. Lauro, C., R. Cipriani, M. Catalano, F. Trettel, G. Chece, V. Brusadin, L. Antonilli, N. van Rooijen, F. Eusebi, B. B. Fredholm, and C. Limatola. 2010. Adenosine A1 receptors and microglial cells mediate CX3CL1-induced protection of hippocampal neurons against Glu-induced death. *Neuropsychopharmacology* 35: 1550–1559.
35. Dénes, A., S. Ferenczi, J. Halász, Z. Környei, and K. J. Kovács. 2008. Role of CX3CR1 (fractalkine receptor) in brain damage and inflammation induced by focal cerebral ischemia in mouse. *J. Cereb. Blood Flow Metab.* 28: 1707–1721.
36. Sabate, J. M., N. Ameziane, J. Lamoril, P. Jouet, J. P. Farmachidi, J. C. Soulé, F. Harnois, I. Sobhani, R. Jian, J. C. Deybach, et al. 2008. The V249I polymorphism of the CX3CR1 gene is associated with fibrostenotic disease behavior in patients with Crohn's disease. *Eur. J. Gastroenterol. Hepatol.* 20: 748–755.
37. McDermott, D. H., J. P. Halcox, W. H. Schenke, M. A. Waclawiw, M. N. Merrell, N. Epstein, A. A. Quyyumi, and P. M. Murphy. 2001. Association between polymorphism in the chemokine receptor CX3CR1 and coronary vascular endothelial dysfunction and atherosclerosis. *Circ. Res.* 89: 401–407.
38. Apostolakis, S., S. Baritaki, G. E. Kochiadakis, N. E. Igoumenidis, D. Panutsopulos, and D. A. Spandidos. 2007. Effects of polymorphisms in chemokine ligands and receptors on susceptibility to coronary artery disease. *Thromb. Res.* 119: 63–71.
39. Apostolakis, S., V. Amanatidou, E. G. Papadakis, and D. A. Spandidos. 2009. Genetic diversity of CX3CR1 gene and coronary artery disease: new insights through a meta-analysis. *Atherosclerosis* 207: 8–15.
40. Stojković, L., T. Djurić, A. Stanković, E. Dinčić, O. Stančić, N. Veljković, D. Alavantić, and M. Zivković. 2012. The association of V249I and T280M fractalkine receptor haplotypes with disease course of multiple sclerosis. *J. Neuroimmunol.* 245: 87–92.
41. Broux, B., K. Pannemans, X. Zhang, S. Markovic-Plese, T. Broekmans, B. O. Eijnde, B. Van Wijmeersch, V. Somers, P. Geusens, S. van der Pol, et al. 2012. CX(3)CR1 drives cytotoxic CD4(+)CD28(−) T cells into the brain of multiple sclerosis patients. *J. Autoimmun.* 38: 10–19.
42. Kruglov, A. A., V. Lampropoulou, S. Fillatreau, and S. A. Nedospasov. 2011. Pathogenic and protective functions of TNF in neuroinflammation are defined by its expression in T lymphocytes and myeloid cells. *J. Immunol.* 187: 5660–5670.
43. Murphy, C. A., R. M. Hoek, M. T. Wiekowski, S. A. Lira, and J. D. Sedgwick. 2002. Interactions between hemopoietically derived TNF and central nervous system-resident glial chemokines underlie initiation of autoimmune inflammation in the brain. *J. Immunol.* 169: 7054–7062.
44. Renno, T., M. Krakowski, C. Piccirillo, J. Y. Lin, and T. Owens. 1995. TNF-alpha expression by resident microglia and infiltrating leukocytes in the central nervous system of mice with experimental allergic encephalomyelitis: regulation by Th1 cytokines. *J. Immunol.* 154: 944–953.
45. Sriram, K., J. M. Matheson, S. A. Benkovic, D. B. Miller, M. I. Luster, and J. P. O'Callaghan. 2006. Deficiency of TNF receptors suppresses microglial activation and alters the susceptibility of brain regions to MPTP-induced neurotoxicity: role of TNF-alpha. *FASEB J.* 20: 670–682.
46. Omari, K. M., and K. Dorovini-Zis. 2003. CD40 expressed by human brain endothelial cells regulates CD4+ T cell adhesion to endothelium. *J. Neuroimmunol.* 134: 166–178.
47. Shrikant, P., I. Y. Chung, M. E. Ballestas, and E. N. Benveniste. 1994. Regulation of intercellular adhesion molecule-1 gene expression by tumor necrosis factor-alpha, interleukin-1 beta, and interferon-gamma in astrocytes. *J. Neuroimmunol.* 51: 209–220.

Downloaded from http://www.jimmunol.org/jimmunol/article-pdf/191/3/1063/1379268/1300040.pdf by guest on 19 April 2024